



# Geophysical study of Ubiaja and Illushi area in northern Anambra basin, Nigeria, using combined interpretation methods of aeromagnetic data

Alexius C. Okorie<sup>1</sup> · Daniel N. Obiora<sup>1</sup> · Emmanuel Igwe<sup>1</sup>

Received: 5 January 2019 / Accepted: 28 March 2019 / Published online: 6 April 2019  
© Springer Nature Switzerland AG 2019

## Abstract

The aeromagnetic data of Ubiaja and Illushi area which falls within latitude 6°30'N–7°00'N and longitude 6°00'N–7°00'E were qualitatively and quantitatively interpreted. The qualitative interpretation revealed that the area is intensely faulted with major anomalies (faults) trending in the northeast and southwest directions. Standard Euler deconvolution, source parameter imaging (SPI) and modeling (forward and inverse) methods were employed in the quantitative interpretation. The aim of the quantitative interpretation includes determination of the thickness of the sedimentary basin, magnetic susceptibilities and possible type of mineralization prevalent in the area. The SPI depth result ranges from – 258.2 to – 3497.7 m. The depth result from standard Euler deconvolution method for the structural index SI=0.5 ranges from 1377.3 to – 2510.9 m; for SI=1, the depth to magnetic sources ranges from 1482.0 to – 3003.3 m; for SI=2, the depth to magnetic sources range from 1627.8 to – 2984.3 m; and for SI=3, the depth ranges from 1853.9 to – 3089.9 m. The results from forward and inverse modeling for profiles 1, 2, 3 and 4 showed depths of – 4118 m, – 3611 m, – 2964 m and – 5489 m, respectively (– signs signify subsurface depth). The susceptibility values of 0.0100 obtained for profiles 1 and 2 are associated with group of minerals such as hematite, gneiss, granite or gabbro. Profile 3 with susceptibility value of 0.0613 is typical of igneous rock porphyry. Profile 4 with susceptibility value of 0.0288 depicts minerals such as slate and hematite.

**Keywords** Aeromagnetic data · Ubiaja and Illushi areas · Rose diagram · Possible minerals · Source parameter imaging (SPI) · Euler deconvolution · Forward and inverse modeling

## Introduction

Minerals and hydrocarbon play vital roles in the socio-economic development of a country. Before the colonial era to the era of the 1960s, the search for mineral deposits and hydrocarbon has been a major business challenge in Nigeria. It is no doubt that the foundation or basis of the Nigerian economy had been the solid minerals, and now the booming oil sector, since over 80% of the nation economy depends greatly on it (Obiora et al. 2015). Since all the exploitation of hydrocarbon in Nigeria is mostly carried out in Niger delta basin, it will benefit the country if other sedimentary basins such as Anambra basin are explored. Anambra basin,

where Ubiaja and Illushi fall, is one of those basins suspected to have hydrocarbon and solid mineral prospect.

Magnetic method is a geophysical survey technique that exploits considerable differences in the magnetic properties of minerals with respect to the ultimate objective of characterizing the earth's subsurface. The technique involves the acquisition of measurements of the amplitude of the magnetic field at discrete points along survey lines distributed regularly throughout the area of interest (Horsfall 1997). Magnetic prospecting, which is the oldest method of geophysical exploration, is used as a reconnaissance tool to explore for hydrocarbon, minerals and even archeological artifacts. In prospecting for oil, it gives information from which one can determine the depth to basement rocks and thus locate and define the extent of sedimentary basins. Another application is the delineation of intra-sedimentary magnetic sources, such as shallow volcanic or intrusive that disrupts the normal sedimentary sequence (Peterson and Reeves 1985). Magnetic surveys may be carried out at sea,

✉ Daniel N. Obiora  
daniel.obiora@unn.edu.ng

<sup>1</sup> Department of Physics and Astronomy, University of Nigeria, Nsukka, Enugu State, Nigeria

in air and on land. The method is broadly used and the technique is very good in the exploration for ore deposits that contain magnetic minerals (Kearey et al. 2002). An aeromagnetic survey permits greater areas of the earth's surface to be covered speedily for regional reconnaissance.

One of the sub-basins in the Benue trough is the Anambra basin (Reijers et al. 1997). The Anambra basin refers to the sedimentary succession that directly overlies the facies of the southern Benue Trough and consists of Campanian to early Paleocene lithofacies. Anambra basin bears several economic earth materials including metalliferous minerals, industrial minerals and rocks, and energy/fuel minerals (Nwajide 2013).

## Geology and stratigraphy of the study area

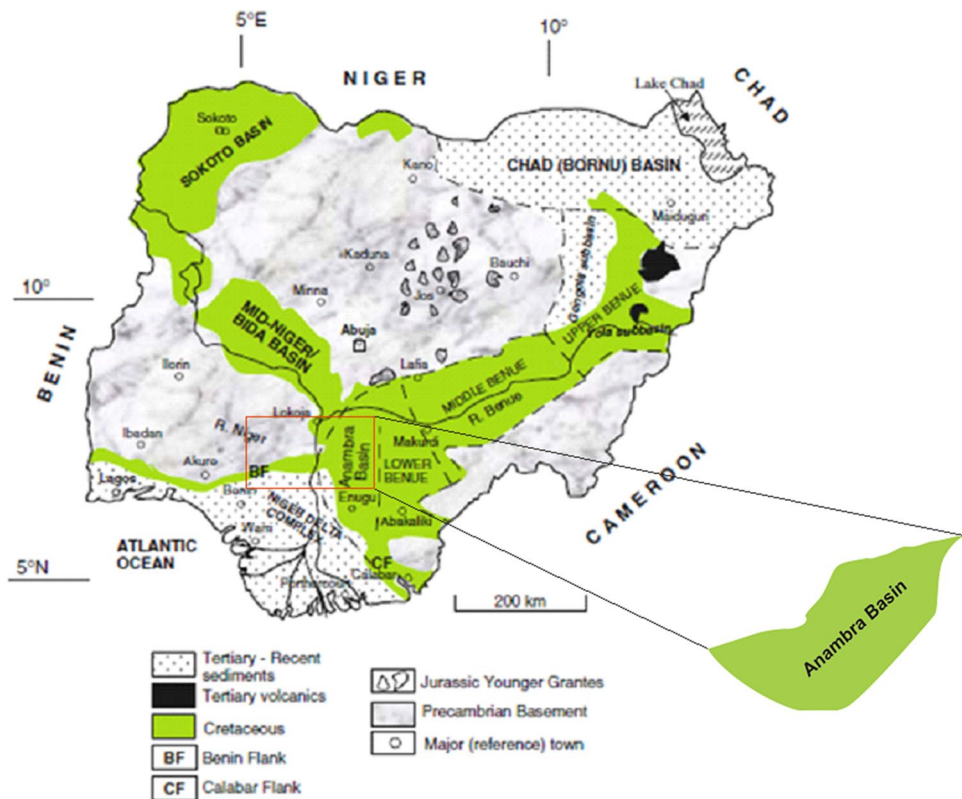
The regional map of Nigeria showing the Anambra basin (Fig. 1) shows the location of some basins with the various formations associated with the basins. The northern Anambra basin within which Ubiaja and Illushi areas fall is located between latitude  $6^{\circ}30'$  and  $7^{\circ}00'N$  and longitude  $6^{\circ}00'$  and  $7^{\circ}00'E$ . The study area covers a total area of about  $6050 \text{ km}^2$  which is situated in the southwestern Nigeria. Ubiaja is located in the Ishan district of Edo state, and is bordered to the south by Benin City, to the southeast by Agbor, to the northeast by Etsako, and to the west by river Niger. Illushi

is located in sub-locality, Illushi locality district, Edo state of Nigeria. Two aeromagnetic maps (sheets 285 and 286) covered the area. The study area consists of two formations and alluvium deposit. These formations include Ameki or Bende-Ameki and Imo shale or Ebenebe sandstone as shown in the detailed geology map of the study area (Fig. 2). Stratigraphically, the Ameki formation overlies the impervious Imo shale group characterized by lateral and vertical variations in lithology. The Imo shale of Paleocene age is underlain in succession by Nsukka formation, Ajali sandstones and Nkporo shales (Reyment 1965).

## Source of data

The study area (Ubiaja and Illushi) is covered by an aeromagnetic survey conducted by Nigerian Geological Survey Agency (NGSA) of Nigeria in 2009. The magnetometer used for the aeromagnetic data survey is '3 × scintrex CS2 Cesium vapor'. The aeromagnetic surveys were flown at 500 m flight line spacing and 5000 m tie line spacing with 75 m sensor mean terrain clearance. The average magnetic inclination for the area is  $-12.7^{\circ}$  while the declination for the area is  $-1.6^{\circ}$ . The geomagnetic gradient was removed from the data collected in digitized form ( $X Y Z$  data). The data collected in digitized format have  $X$  and  $Y$  representing the longitude and the latitude, respectively, while the

**Fig. 1** A regional map of Nigeria showing the Anambra basin (Obaje 2009)



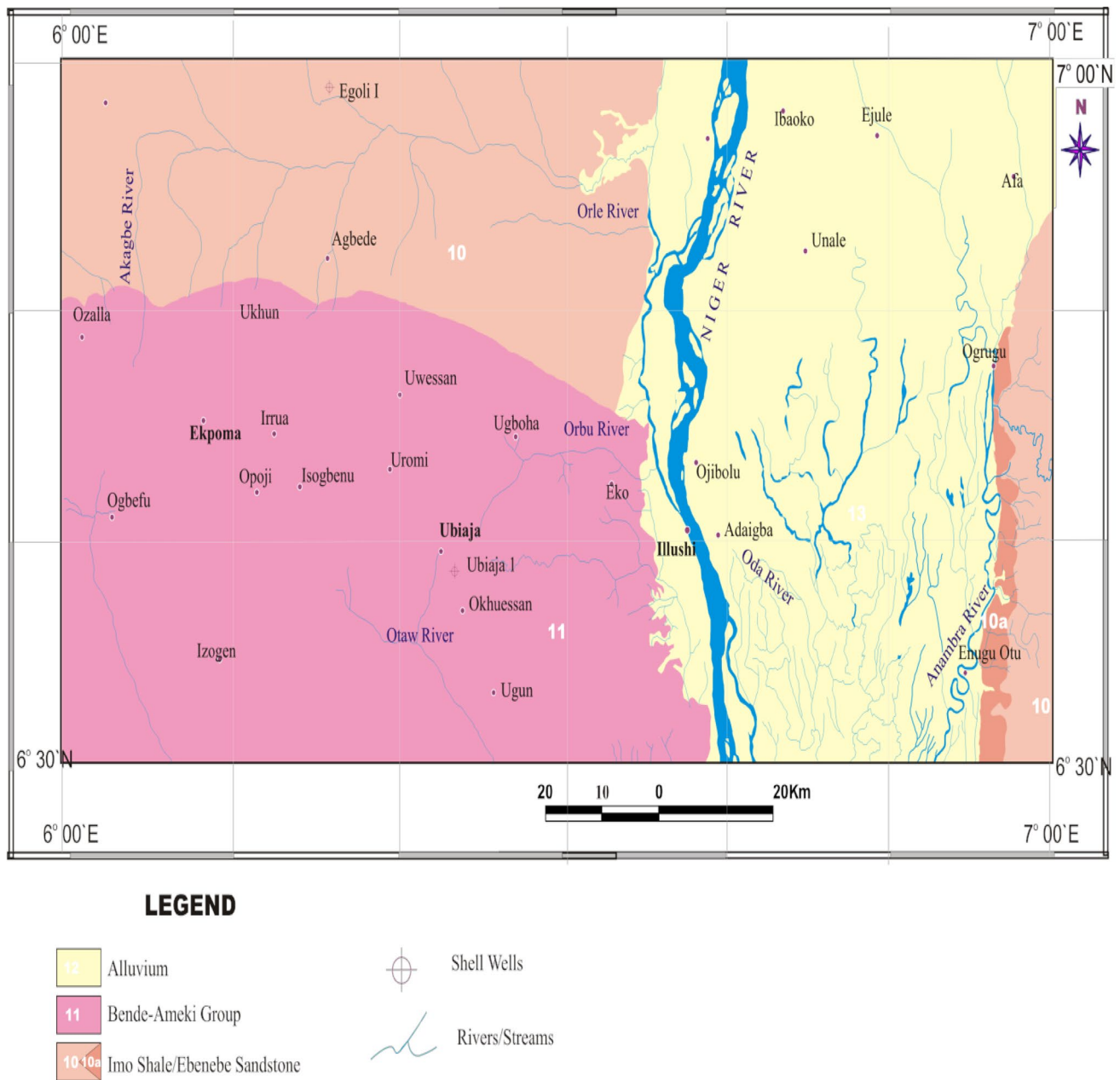


**Fig. 2** Geology map of the study area

Z represents the magnetic intensity measured in nanoTesla (nT). The flight path processing used is the ‘Real Time Differential Global Positioning System (GPS)’.

**Methods and data analysis**

The first step was to merge the two sheets covering the survey area. The data were digitized and provided in excel format which was converted from the excel format to text format. The data in text format were imported to the Oasis

Montaj software and the Total magnetic Intensity map (TMI) was produced. Various filtering processes were applied and maps generated which were exported to the contouring software (Surfer 11). The Rose diagram or the circular histogram was gotten from Rozeta software which shows the structural lineament of the study area. The depths to magnetic source bodies were gotten from the grids of Source Parameter Imaging (SPI), standard Euler deconvolution and modeling methods.

Filtering is done to remove or eliminate noise (unwanted signal). Filtration is a way of separating signals of different

wavelength to isolate and hence, enhance anomalous features with certain wavelength. Oasis Montaj and Surfer 11 software were used in the processing of data in this study. These data processing techniques include gridding, regional–residual separation, first vertical and horizontal derivatives.

The regional anomaly map was separated from residual anomaly map through the application of polynomial fitting to total magnetic intensity. Polynomial fitting of degree 1 was applied to the TMI grid to separate the residual anomaly and regional anomaly maps. The algorithm for the removal of regional field according to Nwankwo (2006) is given as

$$r = a_0 + a_1(X - X_{\text{ref}}) + a_2(Y - Y_{\text{ref}}), \quad (1)$$

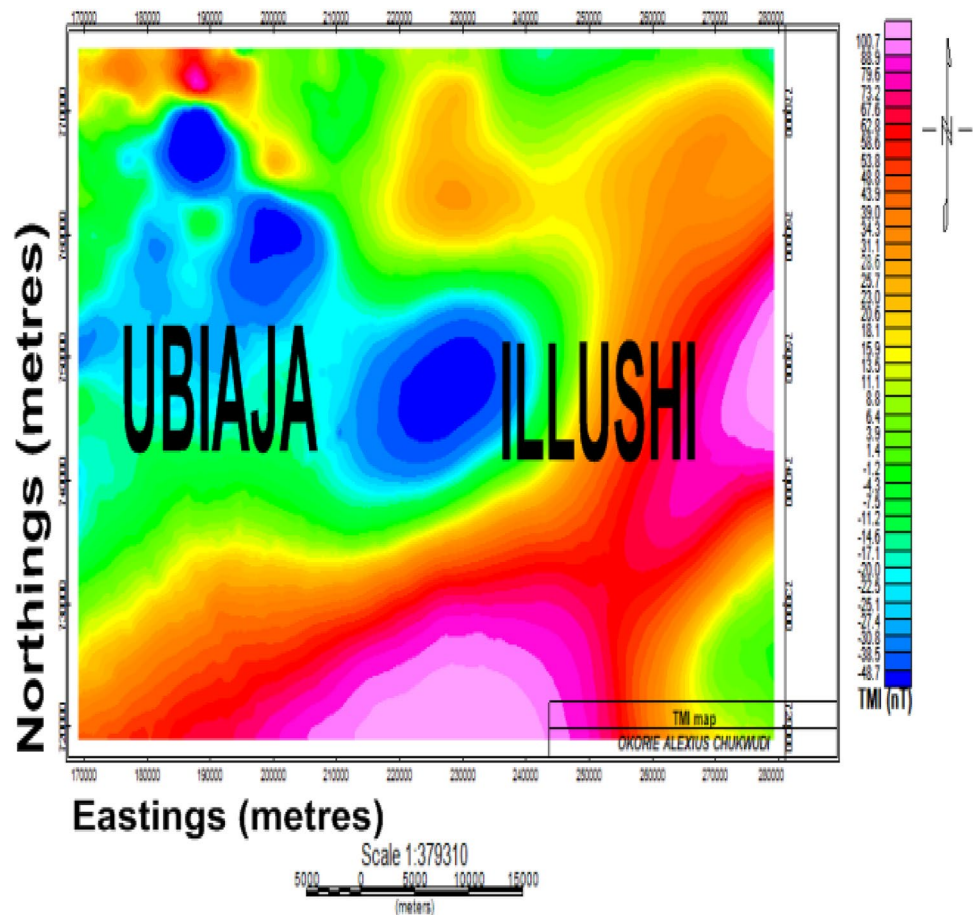
where  $r$  is the regional field,  $X_{\text{ref}}$  and  $Y_{\text{ref}}$  are the  $X$  and  $Y$  coordinates of the geographic center of the data set, respectively. They are used as  $X$  and  $Y$  offsets in the polynomial calculation to prevent high-order coefficients becoming very small,  $a_0$ ,  $a_1$  and  $a_2$  are the regional polynomial coefficients. The residual field is the difference between the observed magnetic (which is the total magnetic intensity) field and the regional field value computed.

The traditional filtering method can either be low pass (regional) or high pass (residual). Regional anomaly is referred to as the component of magnetic anomaly that has higher wavelength. This deep large feature shows up as regional trend and continues smoothly over a wider aerial extent. The residual anomaly has shorter wavelength and

**Table 1** Summary of forward and inverse modeling results

Profiles	$X$ (m)	$Y$ (m)	Depth (m)	Dip (deg.)	Plunge (deg.)	Strike (deg.)	Body shape	$K$ value (SI)	Possible mineral
1	230,493	745,118	– 4118	84.00	– 105.1	– 63.2	Ellipsoid	0.0100	Hematite, gneiss, granite or gabbro
2	226,596	749,478	– 2964	0.0	0.0	– 90.0	Sphere	0.0100	Hematite, gneiss, granite or gabbro
3	202,929	756,298	– 3611	58.8	– 66.6	– 48.4	Ellipsoid	0.0613	Porphyry (igneous rock)
4	274,574	723,582	– 5489	– 77.6	– 89.3	52.0	Ellipsoid	0.0288	Slate or hematite

**Fig. 3** TMI map of the study area



shows up as smaller, local trend which are secondary in size but primary in importance. These residual anomalies may provide structures for mineral ore emplacement. For effective interpretation to take place, the regional and the residual anomalies must be separated. Generally, only the residual or local variations are of interest and hence, interpretation is based on it.

Derivative helps to sharpen the edges of anomaly and enhance shallow features (Telford et al. 1990). This includes first and second vertical derivatives, first horizontal derivative, second horizontal derivative, etc. Computation of the first vertical derivative in an aeromagnetic survey is equivalent to observing the vertical gradient with a magnetic gradiometer with advantages of enhancing shallow sources, suppressing deeper ones and giving a better resolution of closely spaced sources. Hence, the second, third and higher order vertical derivatives can be computed but usually noise in the data becomes more prominent than the signal in the

first vertical derivative because of the Fast Fourier Transform (FFT) used. The FFT is given by

$$F(\omega) = \omega^n \tag{2}$$

This is also calculated noting that a direction (azimuth) needs to be chosen, giving another element of choice for optimum presentation. Alternatively, the maximum horizontal gradient at each grid point can be displayed, regardless of direction.

The horizontal gradient in this work will be filtered in *x*- and *y*-directions (Telford et al. 1990). This method entails removing the dependence of magnetic data on the magnetic inclination, which is converting data which were recorded in the inclined Earth’s magnetic field to what they would have been if the magnetic field had been vertical. This method simplified the interpretation because for sub-vertical prisms or sub-vertical contacts (including faults), it transforms their asymmetric responses to simpler symmetric and anti-symmetric forms. The symmetric “high” are

**Fig. 4** Residual anomaly map of the study area

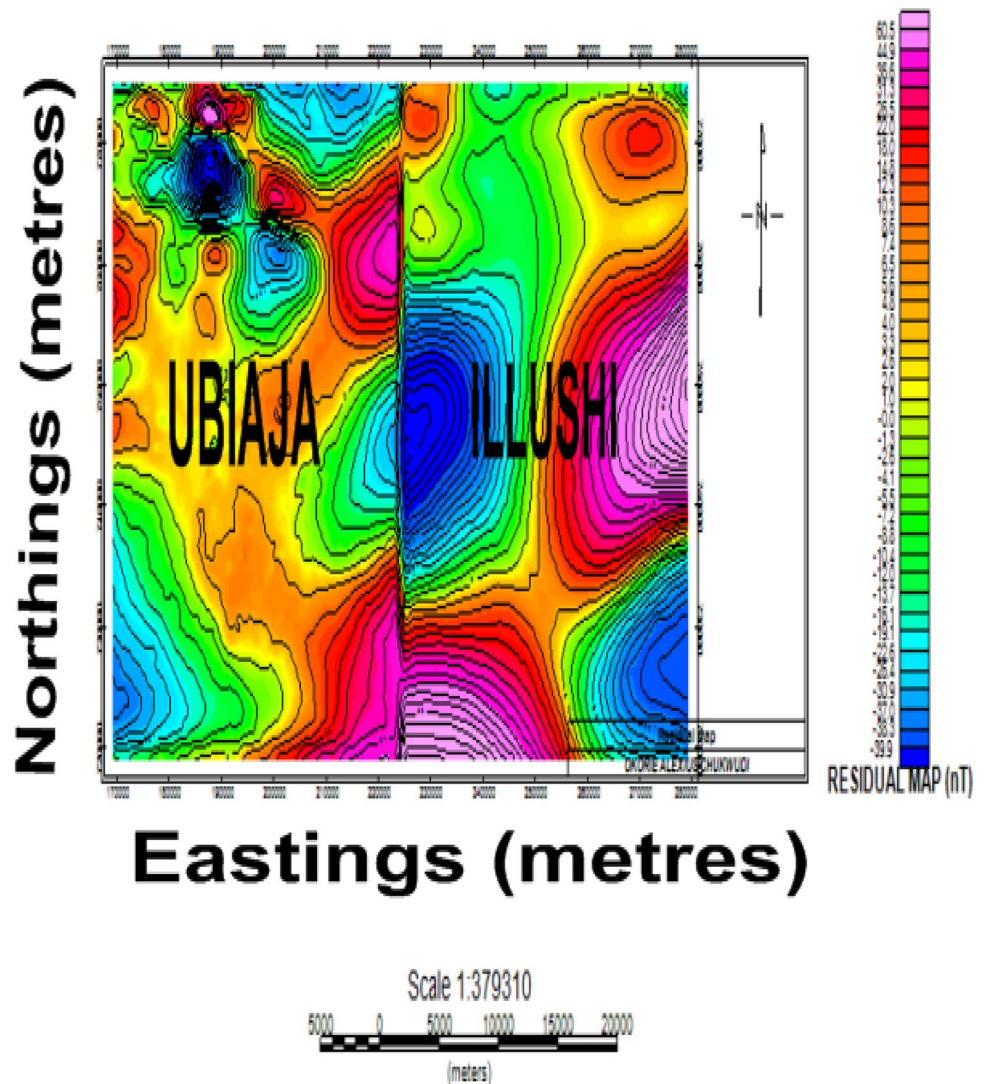
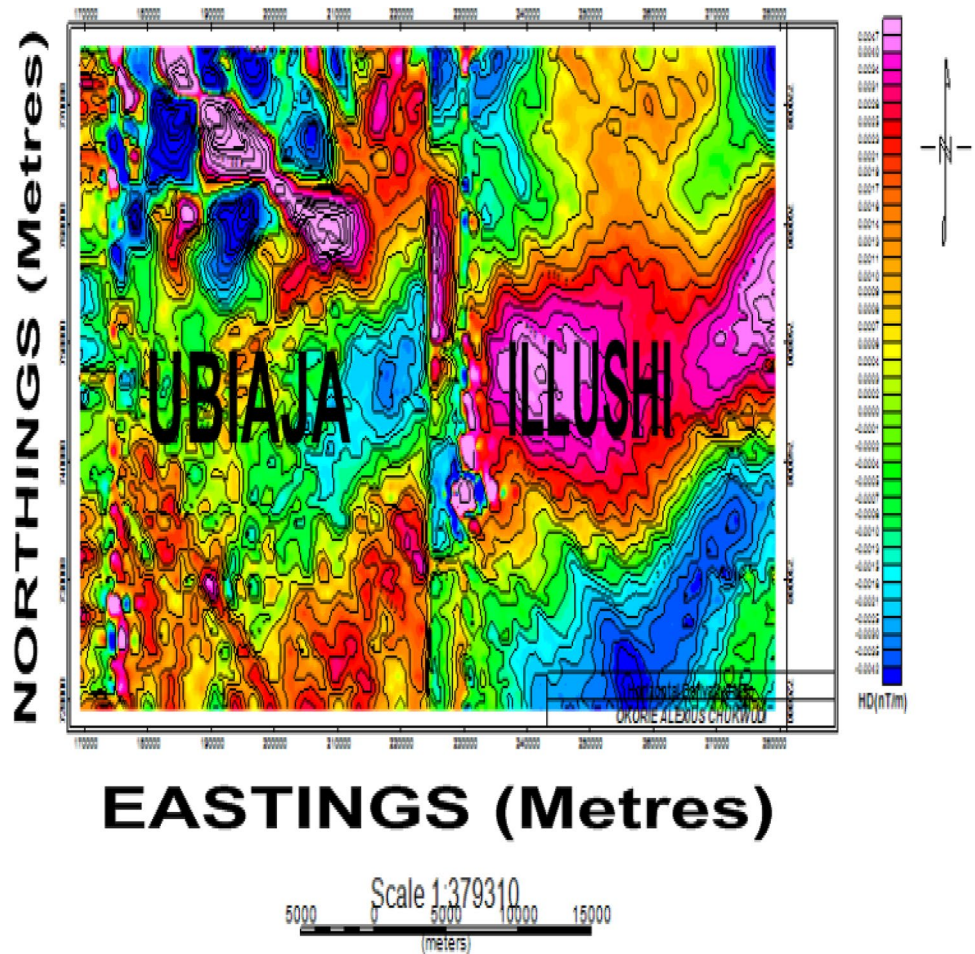


**Fig. 5** First horizontal derivative map



directly centered on the body, while the maximum gradient of the anti-symmetric dipolar anomalies coincides exactly with the body edges.

In the qualitative analysis of the aeromagnetic data of the study area, the Rose diagram was used. The Rose diagram shows the lineation in an area which could be anomalies or faults. In this work, the Rose diagram shows the major and minor anomaly trends.

Source parameter imaging (SPI) is a profile- or grid-based method for estimating magnetic source depths for some source geometries, the dip and susceptibility contrast. The method utilizes the relationship between source depth and the local wave number ( $k$ ) of the observed field, which can be calculated for any point within a grid of data via horizontal and vertical gradients (Thurston and Smith 1997; Fairhead et al. 2004). The fundamentals for SPI are that for vertical contacts, the peaks of the local wave number define the increase of depth. Mathematically,

$$\text{Depth} = \frac{1}{K_{\max}} = \frac{1}{\left( \sqrt{(\partial \text{Tilt} / \partial x)^2 + (\partial \text{Tilt} / \partial y)^2} \right)_{\max}}, \quad (3)$$

where

$$\text{Tilt} = \arctan \left( \frac{\partial T / \partial Z}{\sqrt{(\partial T / \partial X)^2 + (\partial T / \partial Y)^2}} \right) = \arctan \left( \frac{\partial T / \partial Z}{\text{HGRAD}} \right), \quad (4)$$

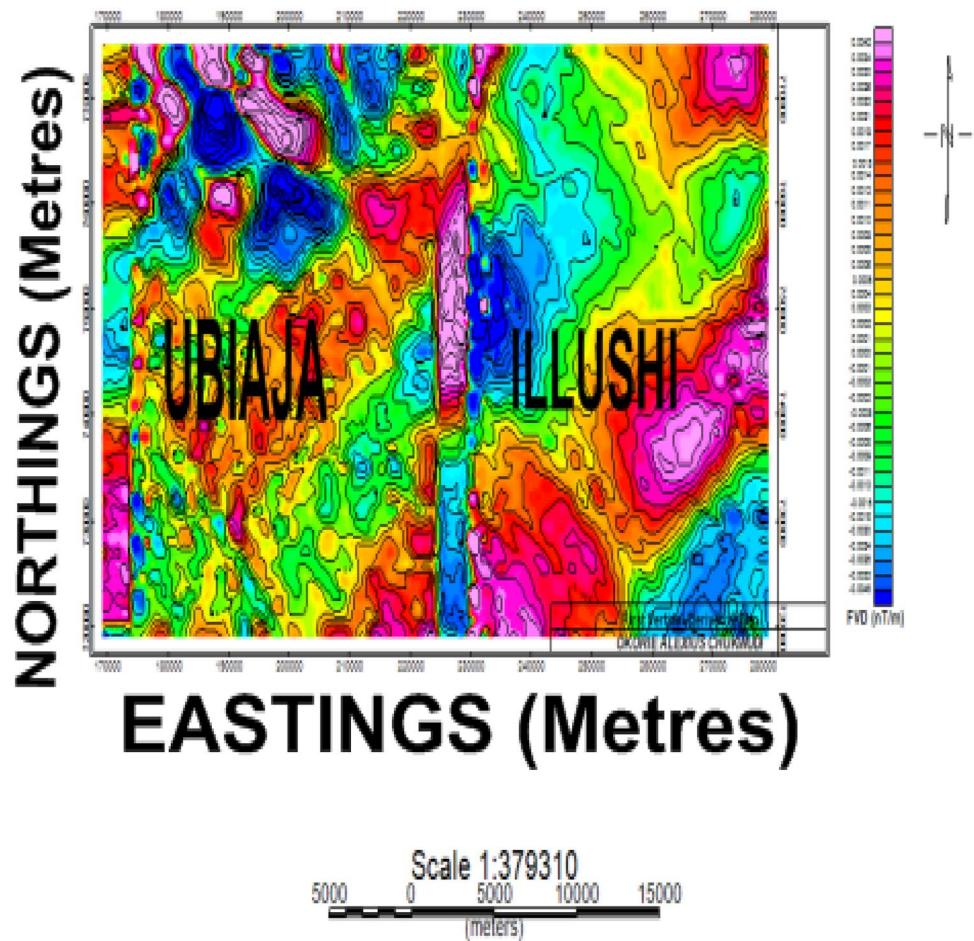
where HGRAD is the horizontal gradient,  $T$  is the total magnetic intensity (TMI),  $\partial T / \partial X$ ,  $\partial T / \partial Y$  and  $\partial T / \partial Z$  are derivatives of  $T$  with respect to  $x$ ,  $y$  and  $z$  (Thurston and Smith 1997). Oasis Montaj software was employed in computing the SPI image and depth.

Euler deconvolution is an interpretation tool in potential field for locating anomalous source and determining their depths using Euler's homogeneity relation (Reid et al. 1990). The homogeneity relation is given as

$$(x - x_0) \frac{\partial T}{\partial x} + (y - y_0) \frac{\partial T}{\partial y} + (z - z_0) \frac{\partial T}{\partial z} = N(B - T), \quad (5)$$

where  $\frac{\partial T}{\partial x}$ ,  $\frac{\partial T}{\partial y}$  and  $\frac{\partial T}{\partial z}$  represent first-order derivative of magnetic field along the  $x$ -,  $y$ - and  $z$ -directions respectively, and  $(x_0, y_0, z_0)$  is the source position of a magnetic source whose

**Fig. 6** First vertical derivative map



total magnetic intensity field,  $T$ , is measured at  $(x, y, z)$ .  $B$  is the regional value of the total field and  $N$  is the structural index. The Euler deconvolution depth estimate was computed using Oasis Montaj software.

Forward and inverse modeling technique was used to further estimate the anomalous source body parameters. Forward modeling involves the comparison of the calculated field of a hypothetical source with that of the observed data. The hypothetical model is adjusted to improve the fit for a subsequent comparison until a perfect or near-perfect fit is obtained. The technique is used to estimate the geometry of the source or the distribution of magnetization within the anomalous source body by trial and error approach. Inverse modeling involves direct determination of some parameters of the source from the measured data. In this method, it is customary to constrain some parameters of the source in some way, realizing that every anomaly has infinite number of permissible sources leading to an infinite number of solutions (Reeves 2005). The potent software which is an extension package of Oasis Montaj software was employed for the modeling and inversion of the anomalies.

## Results

The TMI map is a combination of total signals, both the anomalous and the common signals in an area. The TMI map was produced using Oasis Montaj software. The TMI map (Fig. 3) shows magnetic intensity values ranging from  $-48.7$  to  $100.7$  nT. The area is marked by both high and low magnetic signatures. The circular alignment of blue circular bodies in the northwest and central directions (Fig. 3) in the TMI map suggests that the area could contain intrusive rocks.

The residual anomaly map from polynomial fitting of degree 1 (Fig. 4) shows the magnetic intensity ranging from  $-39.9$  to  $60.5$  nT. The circular-shaped contours found in the northwest and central parts of the study area show areas with low magnetic intensity as indicated by the color legend bar.

The first horizontal derivative map (Fig. 5) shows clearly that the area has low intensity in general as indicated by the color legend bar. The magnetic intensity of the study area ranges from  $-0.0042$  to  $0.0047$  nT/m.

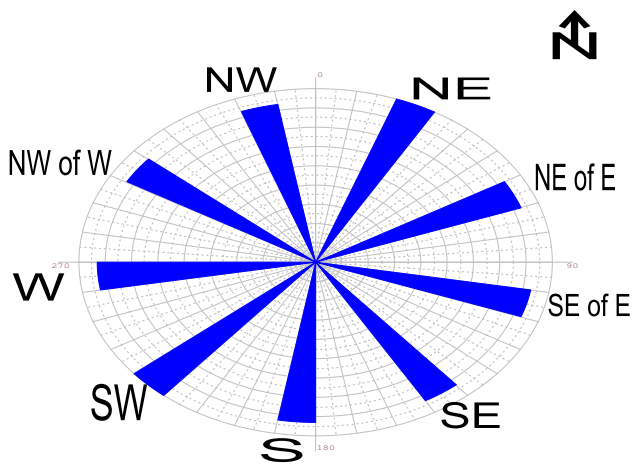
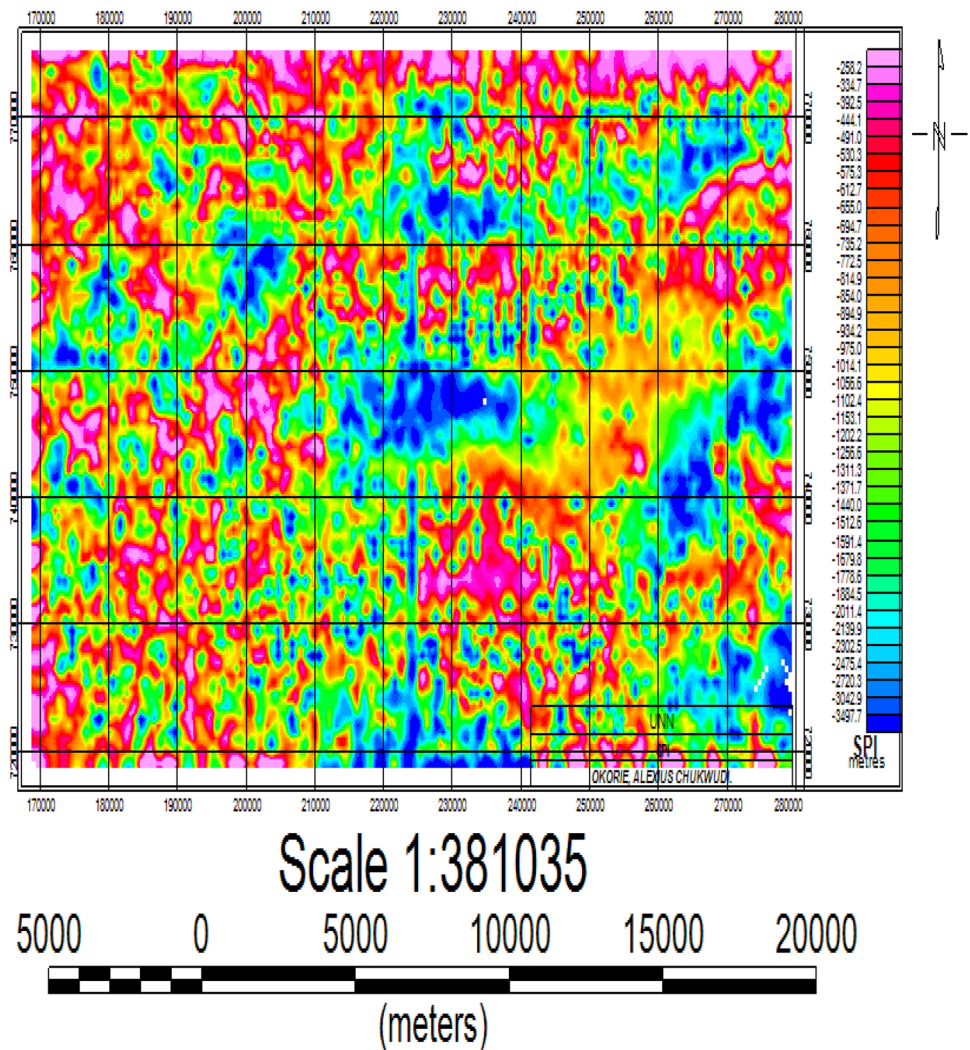


**Fig. 7** Rose diagram of the study area

The first vertical derivative map (Fig. 6) shows the magnetic intensity of the area ranging from  $-0.0048$  to  $0.0042$  nT/m.

**Fig. 8** SPI depth map and legend of the study area



From Fig. 7, the major anomaly trends are northeast (NE) and southwest (SW) directions while the minor anomaly trends are northeast of east (NE of E), southeast (SE), southeast of east (SE of E), south (S), west (W), northwest (NW) and northwest of west (NW of W) directions. The Rose diagram was achieved by the software ROZETA™.

The Oasis Montaj software was used in computing the SPI image and depth. The generated SPI depth map and legend (Fig. 8) shows varied colors supposedly showing different magnetic susceptibility contrast within the study area and could portray the undulations in the basement surface. The negative values indicated in the legend signify depth. The blue colors from the legend show areas of thicker sediments or deep-lying magnetic bodies. The pink, purple, orange and yellow colors at the SPI legend show areas of shallower sediment or near-surface-lying magnetic bodies. The depth of magnetic source ranges from  $-258.2$  to  $-3497.7$  m.

Standard Euler deconvolution (Euler 3-D) interpretation was carried out in three dimensions by employing Oasis Montaj software in the computation of the Euler depth map



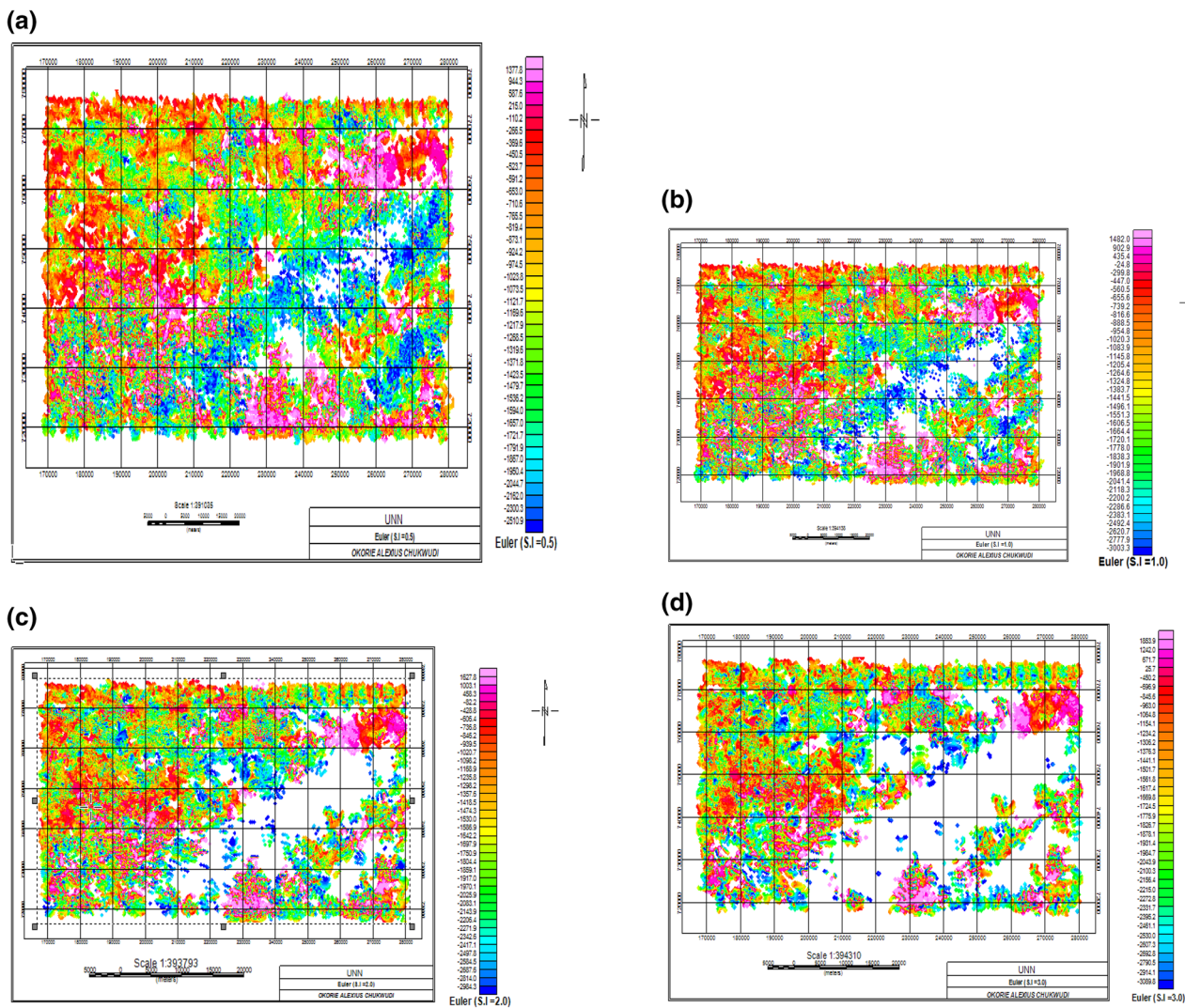


**Fig. 9** a Euler 3D depth and legend (SI=0.5). b Euler 3D depth grid and legend (SI=1.0). c Euler 3D depth grid and legend (SI=2.0). d Euler 3D depth and legend (SI=3.0)

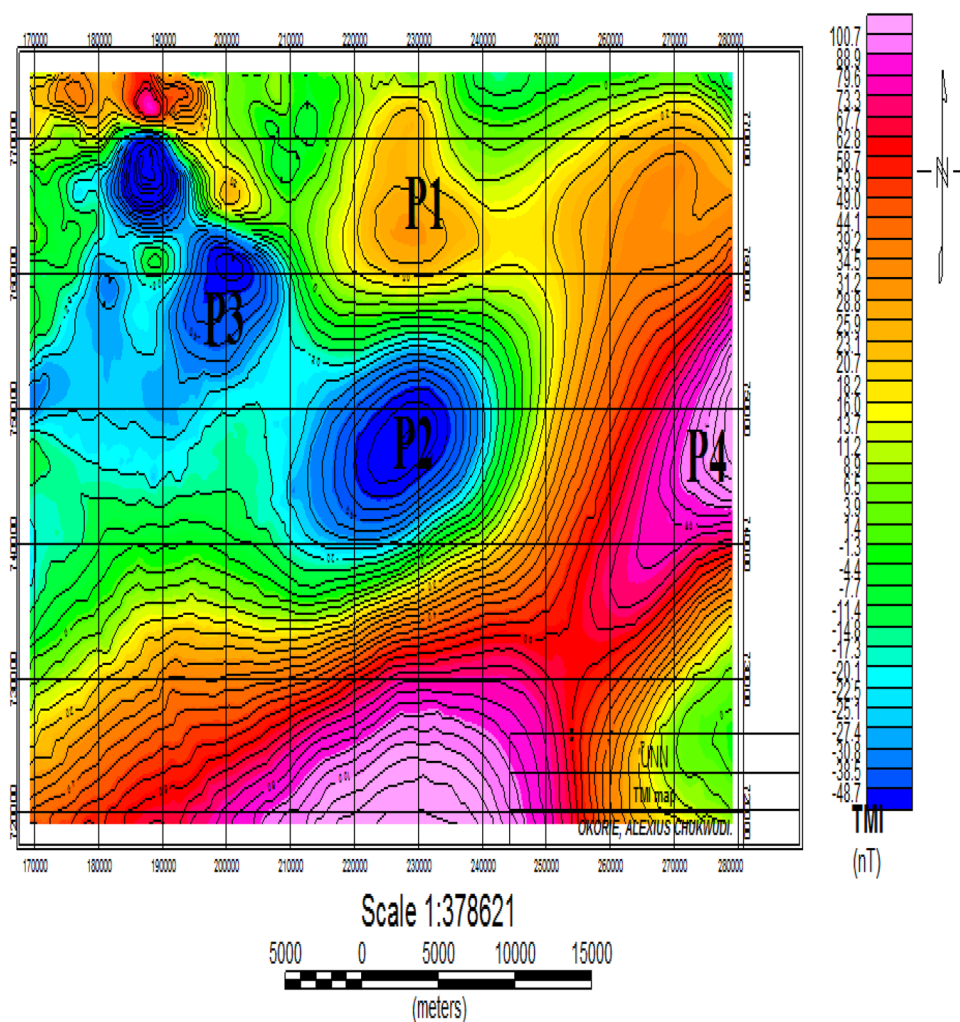
and legend. For four different structural indices (SI=0.5, 1, 2 and 3), four Euler 3D maps were generated (Fig. 9a–d). From the maps, the blue color indicates deep lying magnetic bodies, while the pink color indicates the shallow magnetic bodies. The outcrops as shown by the positive depth values in the color legend bar signify that some parts of the study area are mountainous or rocky, while the negative depth values are depths of deep lying magnetic source bodies. There is no Euler solution (depth) for the particular structural index used as indicated by the areas in the maps without magnetic signatures or color (depth).

The Euler 3D depth grids for structural indices (SI) 0.5, 1, 2 and 3 are shown in Fig. 9a–d, respectively. Depth range for SI=0.5 is from +1377.3 to –2510.9 m; for SI=1, depths range from +1482.0 to –3003.3 m; for SI=2, depths range

from +1627.8 to –2984.3 m; and for SI=3, depths range from +1853.9 to –3089.9 m.

To model the area and find the possible minerals and rocks in the area, four profiles (P1, P2, P3 and P4) were taken at different parts of Fig. 10. From the results (Fig. 11a–d), the blue curves represent the observed field while the red curves represent the calculated fields due to the model. Profiles modeled are chosen if they have good fit and also based on the geology of the area being considered. Profiles P1 and P2 were modeled using ellipsoid and sphere, respectively, and their susceptibility values are both 0.0100 which suggest that the possible bodies causing the anomalies are hematite, gneiss, granite or gabbro (Telford et al. 1990). Profile P3 was modeled using ellipsoid and the susceptibility value is 0.0613 which suggests that the possible body causing the anomaly is porphyry, a hard igneous

**Fig. 10** TMI contoured map showing four profiles



rock made up of feldspar (Telford et al. 1990). The profile P4 was modeled using ellipsoid and the susceptibility is 0.0288 which suggest that the possible bodies causing the anomaly are slate and hematite (Telford et al. 1990). The summary of the modeling results is shown in Table 1.

## Discussion

The qualitative interpretation was done by visual inspection of the total magnetic intensity, residual magnetic anomaly, first vertical derivative, first horizontal derivative and rose diagram maps. The total magnetic intensity ranges from  $-48.7$  to  $100.7$  nT (Fig. 3). Higher values of magnetic intensity were found in the eastern and southern parts of the study area as indicated by the pink color (Fig. 3) and the lower values of magnetic intensity were found in the central and northern parts of the study area as indicated by the blue color. The variation in magnetic intensity could be as a result of degree of strike, variation in depth, difference

in magnetic susceptibility, difference in lithology, dip and plunge. Contour closures seen in the study area suggest the presence of magnetic bodies. The residual anomaly map from polynomial fitting of degree one (Fig. 4) showed magnetic intensity ranging from  $-39.9$  to  $60.5$  nT. The central and the northwestern portions of the map are characterized by low magnetic intensity values or weak anomalies. At the northwest part of the map are smaller magnetic contours which according to Gunn et al. (1997) is an indication of a distinct lithology from the surrounding or possibly a lava flow as evidenced by inhomogeneity of the magnetic units.

The first horizontal derivative map (Fig. 5) showed that the map is characterized by low magnetic source bodies in general. The magnetic intensity of the map is very low in general, ranging from  $-0.0042$  to  $0.0047$  nT/m. The first vertical derivative map (Fig. 6) showed magnetic intensity ranging from  $-0.0048$  to  $0.0042$  nT/m. Higher magnetic intensity values were found in the southern, eastern and northwestern parts of the map. The lower magnetic values were found in the western, northern and central parts of the

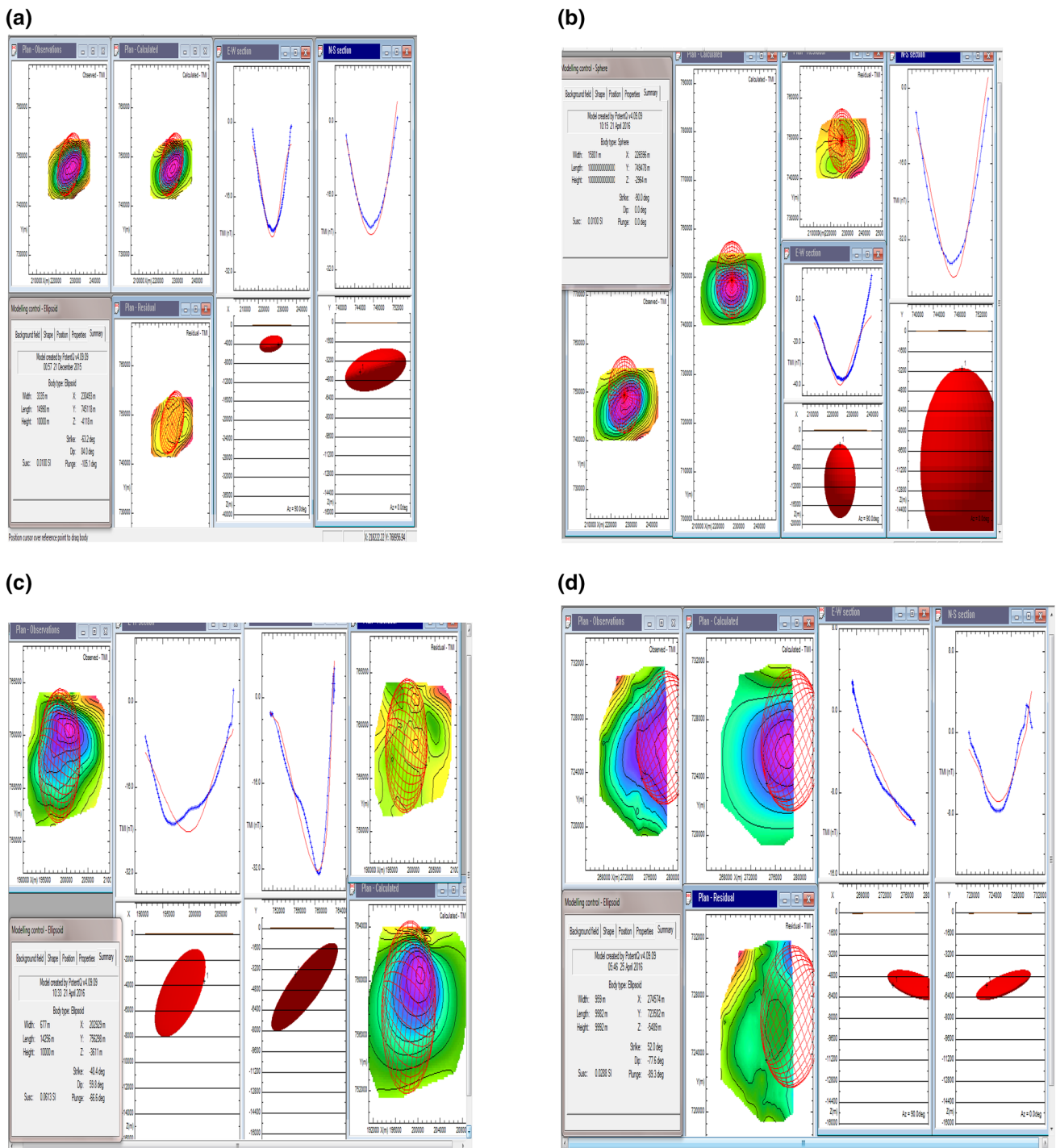


**Fig. 11** **a** Forward and inverse modeling of profile P1. **b** Forward and inverse modeling of profile P2. **c** Forward and inverse modeling of profile P3. **d** Forward and inverse modeling of profile P4

map. The Rose diagram (Fig. 7) showed the structural lineament (fractures, faults, shear zones, veins and foliations) trends. From Fig. 7, one can see the major anomaly trending in the northwest and southwest directions.

The quantitative interpretation was done by numerically determining the depth of shallow and deep magnetic bodies

using Source parameter imaging (SPI), Euler deconvolution and modeling (forward and inverse) methods. The result of SPI depth ranges from  $-258.2$  to  $-3497.7$  m (Fig. 8). The Euler depth grids for various structural indices 0.5, 1, 2 and 3 shown in Fig. 9a–d showed depths ranging from  $+1377.3$  m (outcropping and shallow magnetic bodies) to

- 3089.9 m (deep magnetic source bodies). The study area (Ubiaja and Illushi) is characterized by rocky or mountainous formations. This can clearly be observed from the high positive values from the depth. The depths deduced from the forward and inverse modeling are - 4118 m, - 2964 m, - 3611 m and - 5489 m for profiles 1, 2, 3 and 4, respectively (Fig. 11a–d). The susceptibility values obtained from the model profiles 1, 2, 3 and 4 are 0.0100, 0.0100, 0.0613 and 0.0288, respectively. These susceptibilities values according to Telford et al. (1990) indicates minerals such as hematite, gneiss, granite, gabbro, porphyry or slate and they are all magnetic in nature.

From the three methods employed: SPI, Euler deconvolution and modeling methods, the SPI and Euler 3D deconvolution depths (SI = 1 and 3) are of close range. Depths (thickness) obtained from modeling results (- 2964 m to - 5489 m), SPI (- 258.2 m to - 3497.7 m) and Euler deconvolution (+ 1377.3 m to - 3089.9 m) show thick sediment that is sufficient for hydrocarbon generation and accumulation which agrees with the work of Wright et al. (1985).

## Conclusion

Interpretation of aeromagnetic data of Ubiaja and Illushi areas were carried out qualitatively and quantitatively. In the qualitative interpretation, the sdiagram showed the structural (anomaly) trend in the study area. The major anomaly trends are in the northeast and southwest directions. Source parameter imaging (SPI), standard Euler deconvolution, and modeling (forward and inverse) methods were employed in the quantitative interpretation. The estimated depth from SPI ranges from - 258.2 to - 3497.7 m. The Euler 3D depth grids for structural indices (SI) 0.5, 1, 2 and 3 are shown in Fig. 9a–d. Depth range for SI = 0.5 is from + 1377.3 to - 2510.9 m; for SI = 1, depths range from + 1482.0 to - 3003.3 m; for SI = 2, depths range from + 1627.8 to - 2984.3 m; and for SI = 3, depths range from + 1853.9 to - 3089.9 m. The susceptibility values obtained from the model profiles 1, 2, 3 and 4 are 0.0100, 0.0100, 0.0613 and 0.0288, respectively, which indicate dominance of paramagnetic minerals (as indicated by positive susceptibility values) such as hematite, gneiss, granite, gabbro, porphyry and slate. Results from SPI, forward and inverse modeling and standard Euler deconvolution methods show that the study area has sedimentary thickness that is suitable for hydrocarbon generation and accumulation. This study has greatly helped

to delineate geophysical structures and has revealed the possible solid mineral potentials of the study area.

**Acknowledgements** The authors are grateful to the Editor, the Editorial Board members and the reviewers for doing a great and meticulous work which helped to improve the quality of this article.

## References

- Fairhead JD, Williams SE, Flanagan G (2004) Testing magnetic local wavenumber depth estimation methods using a complex 3D test model. Society of Exploration Geophysicists Annual Meeting, Denver, Extended Abstract
- Gunn PJ, Maidment D, Milligan PR (1997) Interpreting aeromagnetic data in areas of limited outcrops. *J Aust Geol Geophys* 17(2):175–185
- Horsfall KR (1997) Airborne magnetic and gamma-ray data acquisition. *AGSO J Geol Geophys* 17:23–30
- Kearey P, Brooks M, Hill I (2002) An introduction to geophysical exploration (3rd edition). T.J International, Padstow, Cornwall, Hong Kong
- Nwajide CS (2013) Geology of Nigeria's sedimentary basins. CSS Bookshops, Lagos
- Nwankwo LI (2006) A least square plane surface polynomial fit of two dimensional potential field geophysical data using Matlab. *Nigeria J Pure Appl Sci* 21:2006–2013
- Obaje NG (2009) Geology and mineral resources of Nigeria. Springer, Berlin
- Obiora DN, Ossai MN, Okwoli E (2015) A case study of aeromagnetic data interpretation of Nsukka area, Enugu state, Nigeria, for hydrocarbon exploration. *Int J Phys Sci* 10(17):503–519
- Peterson JR, Reeves CV (1985) Application of gravity and magnetic surveys. The state-of-the art in 1985. *Geophysics* 50:2558–2594
- Reeves C (2005) Aeromagnetic Surveys; Principles. Practice and Interpretation, GEOSOFT
- Reid AB, Allsop JM, Granser H, Millett AJ, Somerton IW (1990) Magnetic interpretation in three dimensions using Euler deconvolution. *Geophysics* 55:80–91
- Reijers TJA, Petters SW, Nwajide CS (1997) The Niger Delta Basin. In: Selley RC (ed) *African Basins*. Elsevier, Amsterdam, pp 151–172
- Reyment RA (1965) Aspect of the geology of Nigeria. Ibadan University Press, Ibadan
- Telford WM, Geldart LP, Sheriff RE (1990) *Applied Geophysics*, 2nd edn. Cambridge University Press, Cambridge
- Thurston JB, Smith RS (1997) Automatic conversion of magnetic data to depth, dip and susceptibility contrast using the SPI method. *J Geophys* 62(3):307–813
- Wright JB, Hastings D, Jones WB, Williams HR (1985) Geology and mineral resources of West Africa. George Allen and Urwin, London

**Publisher's Note** Springer Nature remains neutral with regard to jurisdictional claims in published maps and institutional affiliations.